Electronic Supporting Information

Exploring Polymorphism, Stoichiometric Diversity and Simultaneous Existence of Salt and Cocrystal During Cocrystallization Using Mechanochemistry

Diptajyoti Gogoi,[1] Kalyan J. Kalita,[2] Nishant Biswakarma,[3] Mihails Arhangelskis,[4] Ramesh Ch Deka*,[3] and Ranjit Thakuria*,[1]

[1] Department of Chemistry, Gauhati University, Guwahati 781014, India

[2] Department of Chemical Sciences, Indian Institute of Science Education and Research Kolkata, 741246, West Bengal, India

[3] Department of Chemical Sciences, Tezpur University, Tezpur, Assam, India

[4] Faculty of Chemistry, University of Warsaw, 1 Pasteura Street, 02-093 Warsaw, Poland.

Table of Contents

1. Cambridge Crystallographic Database (CSD) Survey

The CSD search has been conducted using ConQuest Version 5.13. in the software, there is polymorphic subset with 39,741 hits. Only crystal structures containing the keyword "polymorph" (*i.e.* the compound was described in the literature as being polymorphic) were kept.

Additional filters which were used:

- 3D coordinates determined;
- no ions;

- no powder structures;
- not polymeric;

from this search, we got 15,770 hits. Out of which 269 are cocrystals including 6 cocrystals hydrate and only 5 cocrystal hydrates are reported which have report on polymorphs.

Table S1: list of so far reported cocrystals hydrate.

S.No.	REFERENCE/DOI	Refcode	Z''
1.	C.Fiore, A.Baraghini, O.Shemchuk, V.Sambri, M.Morotti, F.Grepioni, D.Braga, *Cryst.Growth Des*. ,**2022**, 22, 1467 (10.1021/acs.cgd.1c01435)	QANXAI, QANXAI01	9, 9
2.	S.Aitipamula, A.B.H.Wong, Pui Shan Chow, R.B.H.Tan, *CrystEngComm* ,**2013**, 15, 5877 (10.1039/C3CE40729B)	BICQUB, BICQUB01	3, 6
3.	M.V.Sosa-Rivadeneyra, P.Venkatesan, F.Flores-Manuel, S.Bernes, H.Hopfl, M.Ceron, S.Thamotharan, M.Judith Percino,*CrystEngComm*,**2020**, 22, 6645 (10.1039/D0CE01056A)	CUWPES, CUWPES01	3, 3
4.	M.K.Chantooni Junior, D.Britton, I.M.Kolthoff, *J.Crystallogr.Spectrosc.Res.,***1993**, 23, 497 (10.1007/BF01182526)	YAXCEF, YAXCEF01	5, 5
5.	B. Zhou, Q. Zhao, L. Tang, D. Yan, Chem.Commun., **2020**, 56, 7698 (10.1039/D0CC02730H)	ZUSPIP, ZUSPIP01	4, 8

Table S2. Crystallographic parameters of the TACA-NA multicomponent solids

Compound name	**TACA•NA molecular salt monohydrate (1:1:1)**	**TACA•NA molecular salt monohydrate (1:1:1)**	**TACA•NA cocrystal monohydrate (2:4:1) Form I**	**TACA•NA cocrystal monohydrate (2:4:1) Form II**
Chemical formula	$C_6H_5O_6$•$C_6H_7N_2O$•H_2O	$C_6H_5O_6$•$C_6H_7N_2O$•H_2O	2($C_6H_6O_6$)•4($C_6H_6N_2O$)•H_2O	2($C_6H_6O_6$)•4($C_6H_6N_2O$)•H_2O
M_r	314.25	314.25	854.74	854.74
Crystal system	Monoclinic	Monoclinic	Triclinic	Triclinic

Space group	*Cc*	*Cc*	$P\bar{1}$	$P\bar{1}$
Temperature (K)	296	100	296	296
a (Å)	12.9786 (15)	12.8183(3)	5.0306 (9)	5.0668 (7)
b (Å)	5.1427 (6)	5.1324(2)	14.977 (3)	17.993 (3)
c (Å)	20.843 (3)	20.7423(6)	26.812 (5)	22.139 (3)
α (°)	90	90	84.727 (5)	92.134 (5)
β (°)	102.570 (3)	103.769(3)	87.615 (5)	93.962 (4)
γ (°)	90	90	87.464 (5)	94.232 (4)
V (Å^3)	1357.8 (3)	1325.39(7)	2008.2 (6)	2006.2 (5)
Z	4	4	2	2
Radiation type	Mo *K*α	Cu *K*α	Mo *K*α	Mo *K*α
μ (mm^{-1})	0.13	1.17	0.11	0.11
Density (g cm^{-3})	1.537	1.575	1.414	1.415
Diffractometer	Bruker *APEX*-II CCD	XtaLAB Synergy, Dualflex, HyPix	Bruker *APEX*-II CCD	Bruker *APEX*-II CCD
Absorption correction	Multi-scan Bruker AXS *SADABS* program	Multi-scan CrysAlis PRO 1.171.42.88a (Rigaku Oxford Diffraction, 2023)	Multi-scan Bruker AXS *SADABS* program	Multi-scan Bruker AXS *SADABS* program
No. of measured reflections	9970	3701	60538	74875
No. of independent reflections	2752	1920	8337	10939
No. of observed [$I > 2\sigma(I)$] reflections	2665	1913	5906	6550
R_{int}	0.022	0.023	0.063	0.083
$(\sin\theta/\lambda)_{max}$ (Å^{-1})	0.635	0.633	0.631	0.694
$R[F^2 > 2\sigma(F^2)]$	0.028	0.028	0.050	0.062
$wR(F^2)$	0.069	0.073	0.151	0.184
S	1.03	1.05	1.04	1.02

$\Delta\rho_{max}$, $\Delta\rho_{min}$ (e Å^{-3})	0.14, −0.20	0.16, −0.17	0.53, −0.25	0.47, −0.27
CCDC No.	2291739	2355242	2291740	2291741

2. Table S3. Hydrogen bond parameters of the TACA-NA multicomponent solids

Interaction	**D–H (Å)**	**H···A (Å)**	**D···A (Å)**	**D–H···A (degree)**	**Symmetry code**
TACA•NA molecular salt monohydrate (1:1:1) at 296 K					
O4–H4A···O8	0.813	1.780	2.591	175.58(1)	x, y, z
N2–H7A···O6	0.999	1.568	2.566	175.49(1)	x, y, z
N2–H7A···O7	0.999	2.524	3.197	124.46(1)	x, y, z
N1–H1A···O5	0.879	2.082	2.942	166.02(1)	x-1/2, +y-1/2, +z
O2–H2A···O1	0.857	1.813	2.670	178.70(1)	x+1/2, -y+1/2, +z+1/2
O8–H8B···O3	0.819	2.002	2.808	167.87(1)	x+1/2, +y-1/2-1, +z
O8–H8A···O6	0.869	1.895	2.755	170.58(1)	x+1/2, +y-1/2, +z
N1–H1B···O7	0.857	1.963	2.811	170.04(1)	x-1/2, +y-1/2-1, +z
TACA•NA molecular salt monohydrate (1:1:1) at 100 K					
N2–H2B···O6	1.08(3)	1.47(4)	2.552(3)	175(4)	x, y, z
N2–H2B···O7	1.08(3)	2.48(4)	3.167(3)	120(2)	x, y, z
O4–H4A···O8	0.80(4)	1.77(4)	2.570(3)	176(3)	x, y, z
N1–H1A···O7	1.00(4)	1.78(4)	2.774(3)	174(3)	1/2+x,-3/2+y,z
N1–H1B···O5	0.91(3)	2.02(3)	2.922(3)	170(3)	1/2+x,-1/2+y,z
O2–H2A···O1	0.83(4)	1.83(4)	2.653(3)	173(4)	-1/2+x,1/2-y,-1/2+z
O8–H8B···O3	0.81(4)	2.00(4)	2.783(3)	164(4)	-1/2+x,-3/2+y,z
O8–H8A···O6	0.86(4)	1.86(4)	2.720(3)	179(6)	-1/2+x,-1/2+y,z
TACA•NA cocrystal monohydrate (2:4:1) Form I					
O11–H11A···N2	0.985	1.651	2.629	170.97(2)	x, y, z
O17–H17B···O12	0.868	1.927	2.791	173.26(2)	x, y, z
N1–H1A···O9	0.911	2.639	3.246	124.80(2)	x, y, z

N1–H1B···O17	0.853	2.401	3.228(1)	163.43(2)	x, y, z
N3–H3B···O17	0.861	2.230	3.053	159.89(2)	x, y, z
O16–H16A···N4	0.946	1.667	2.612	177.54(2)	x+1, +y, +z
O5–H5C···N1	0.879	2.983	3.701	140.16(2)	x+1, +y, +z
O5–H5C···O1	0.879	1.725	2.596	170.66(2)	x+1, +y, +z
N7–H7A···O4	0.920	2.254	3.147(1)	163.42(2)	x+1, +y, +z
N3–H3A···O9	0.936	1.965	2.879	164.91(2)	x+1, +y, +z
O17–H17A···O15	0.955	2.002	2.896	154.98(2)	x-1, +y, +z
O14–H14A···N6	0.913	1.753	2.665	176.91(2)	x-1, +y, +z
O10–H10A···O2	0.909	1.713	2.616	171.64(2)	x-1, +y, +z
O10–H10A···N3	0.909	2.893	3.602	136.01(2)	x-1, +y, +z
N1–H1A···O6	0.911	2.048	2.906	156.44(2)	x-1, +y, +z
N7–H7B···O7	0.857	2.133	2.971	165.52(2)	-x, -y+1, -z+1
N5–H5A···O2	0.900	2.537	3.346	149.90(2)	x-1, +y+1, +z
O8–H8A···N8	1.088	1.505	2.587	171.71(2)	x-1, +y-1, +z
N5–H5B···N5	0.978	2.960	3.694(1)	132.72(2)	-x, -y+2, -z+2
N5–H5B···O3	0.978	1.914	2.891	177.81(2)	-x, -y+2, -z+2
TACA•NA cocrystal monohydrate (2:4:1) Form II					
N2–H2B···O17	0.896	2.441	3.222	145.76(1)	x, y, z
N4–H4A···O5	0.900	2.608	3.176	121.81(1)	x, y, z
N4–H4B···O17	0.893	2.246	3.129	169.95(2)	x, y, z
O11–H11C···N3	0.944	1.710	2.645	170.21(2)	x, y, z
O17–H17B···O12	0.912	1.976	2.870	166.32(2)	x, y, z
O1–H1A···N7	1.096	1.510	2.604	174.88(2)	x+1, +y-1, +z
O3–H3A···N4	1.022	2.968	3.782	137.25(1)	x-1, +y, +z
N6–H6B···O15	0.943	2.124	3.047	165.59(1)	x-1, +y, +z
N8–H8B···O16	0.904	2.051	2.881	152.20(1)	x-1, +y, +z
O3–H3A···O14	1.022	1.569	2.581	169.63(2)	x-1, +y, +z
O10–H10A···N1	1.009	1.638	2.644	175.48(1)	x-1, +y, +z
N2–H2A···O5	0.966	1.940	2.889	166.76(2)	x-1, +y, +z
N2–H2B···O13	0.896	2.948	3.518	123.07(1)	x+1, +y, +z
O7–H7A···N5	1.043	1.622	2.662	175.67(1)	x+1, +y, +z
N4–H4A···O4	0.900	2.113	2.966	157.74(1)	x+1, +y, +z

O6–H6C···N2	0.909	2.933	3.633	135.03(2)	x+1, +y, +z
O6–H6C···O13	0.909	1.755	2.659	173.18(2)	x+1, +y, +z
O17–H17A···O9	0.904	2.133	2.885	140.07(2)	x+1, +y, +z
N6–H6A···O1	0.850	2.584	3.175	127.67(1)	x-1, +y+1, +z
N6–H6A···O3	0.850	2.528	3.275	147.19(2)	x, +y+1, +z
N8–H8A···O2	0.866	2.006	2.867	172.91(1)	-x+1, -y+1, -z

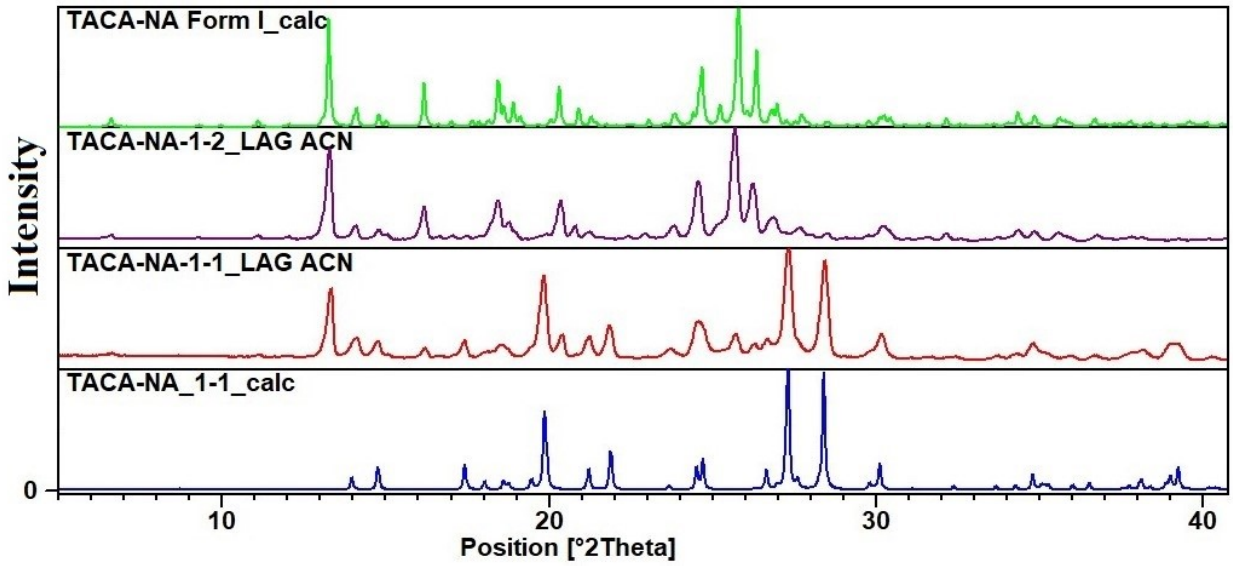

Figure S1. Comparison of experimental PXRD patterns of 1:1 and 1:2 TACA-NA mixture with simulated powder patterns of 1:1 (TACA)•(NA)•(H_2O) salt hydrate and 1:2 $(TACA)_2$•$(NA)_4$•(H_2O) Form I.

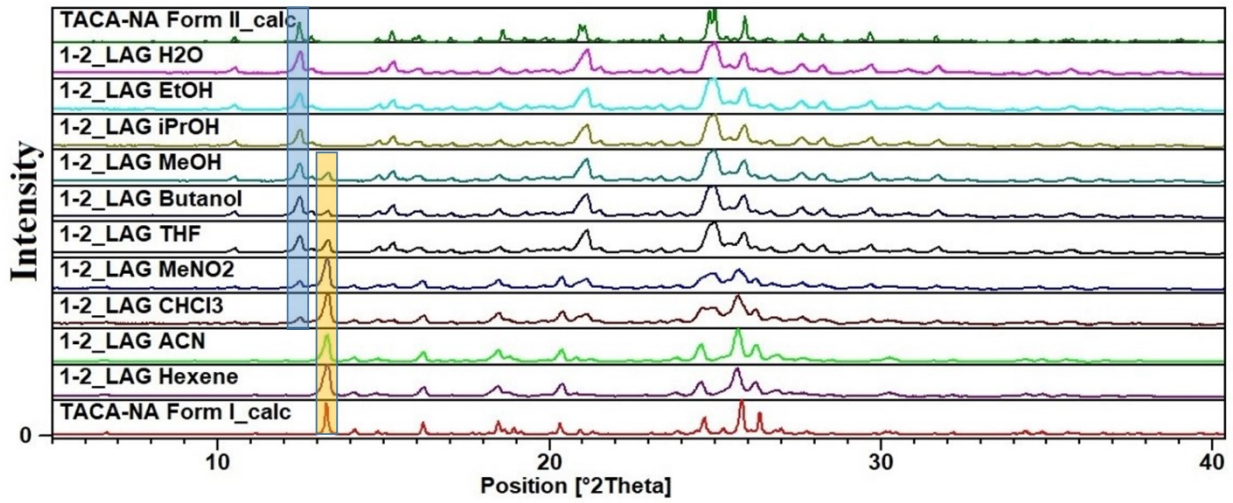

Figure S2. Experimental PXRD patterns of 1:2 TACA-NA ground powder in presence of various added liquids. PXRD pattern of (TACA)•(NA)•(H_2O) salt hydrate ground in presence of various added liquids. Formation of respective polymorphs has been confirmed based on the characteristic peaks of Form I and II highlighted by yellow and blue lines respectively.

For 1:1 (TACA)•(NA)•(H_2O) salt hydrate, the peak at 3511.11 cm^{-1} corresponds to the N-H stretching of the amide group and peak at 3401.63 corresponds to the N-H stretching of the pyridinium ring of nicotinamide.[1] Which implies that a proton is transferred from one of the carboxylic acid groups of TACA to the ring nitrogen of NA. Again, we also observed a shift of wave number from 1708.65 (or 1708.52) cm^{-1} for $(TACA)_2$•$(NA)_4$•(H_2O) Form I (or Form II) to 1696.74 cm^{-1} for 1:1 (TACA)•(NA)•(H_2O) salt hydrate which corresponds to C=O of carboxylic group of TACA. The shift is observed because of the formation of carboxylate ion after proton transfer. O-H stretching frequency of the carboxylic acid groups of TACA for all the multi-component solids are unique, broad and observed within 2700-3300 cm^{-1} well separated from the N-H stretching region. However, it is difficult to conclude, as TACA-NA system has multiple carboxylic acid functions (for TACA) and amide functional groups (for NA) that create difficulty in interpretation of the FT-IR spectra. Therefore, SCXRD analysis would be a better approach to characterize formation of salt vs. cocrystal for similar systems.

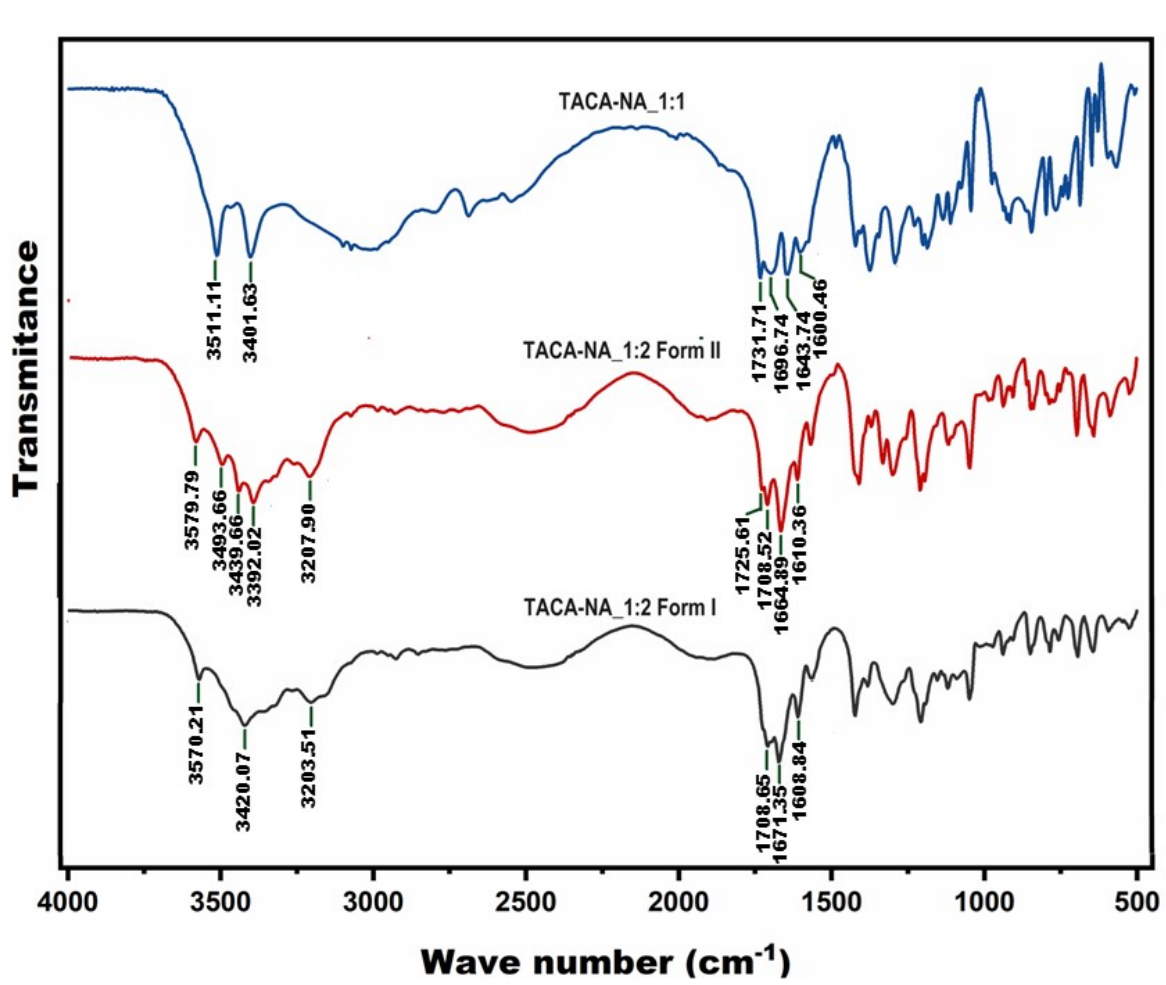

Figure S3. FT-IR spectra of 1:1 (TACA)•(NA)•(H_2O) salt hydrate, 1:2 $(TACA)_2$•$(NA)_4$•(H_2O) Form I and 1:2 $(TACA)_2$•$(NA)_4$•(H_2O) Form II cocrystals.

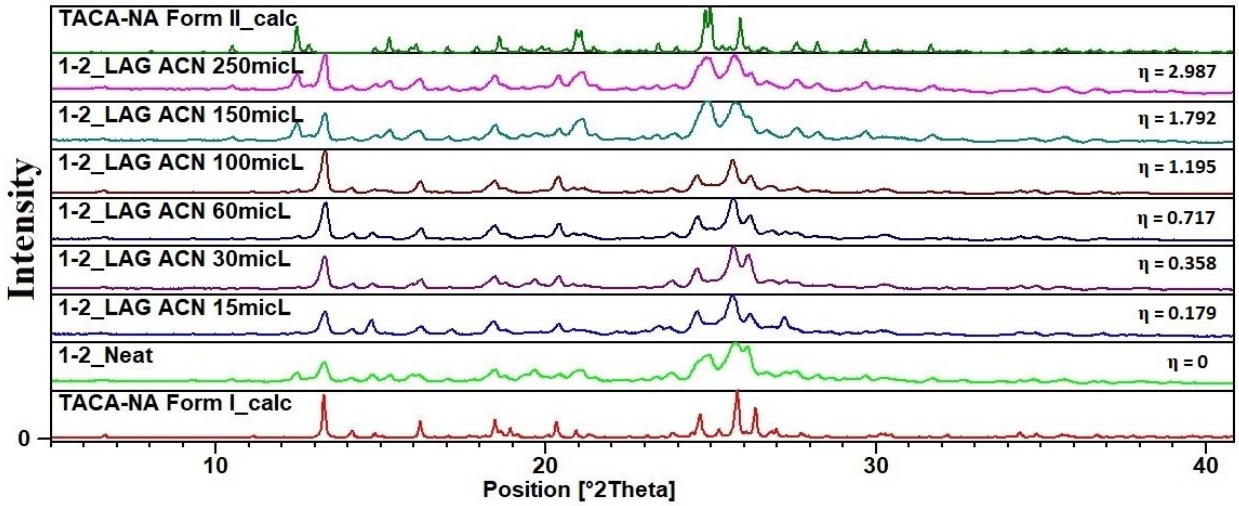

Figure S4. PXRD pattern of 1:2 TACA-NA mixture ground in presence of different amount of ACN. Formation of concomitant mixture (Form I and II) above η value of 1.196 was confirmed based on presence of 2θ peak at 12.5 characteristic of Form II.

3. PXRDs of all the TACA-NA multicomponent solids in turnover experiments

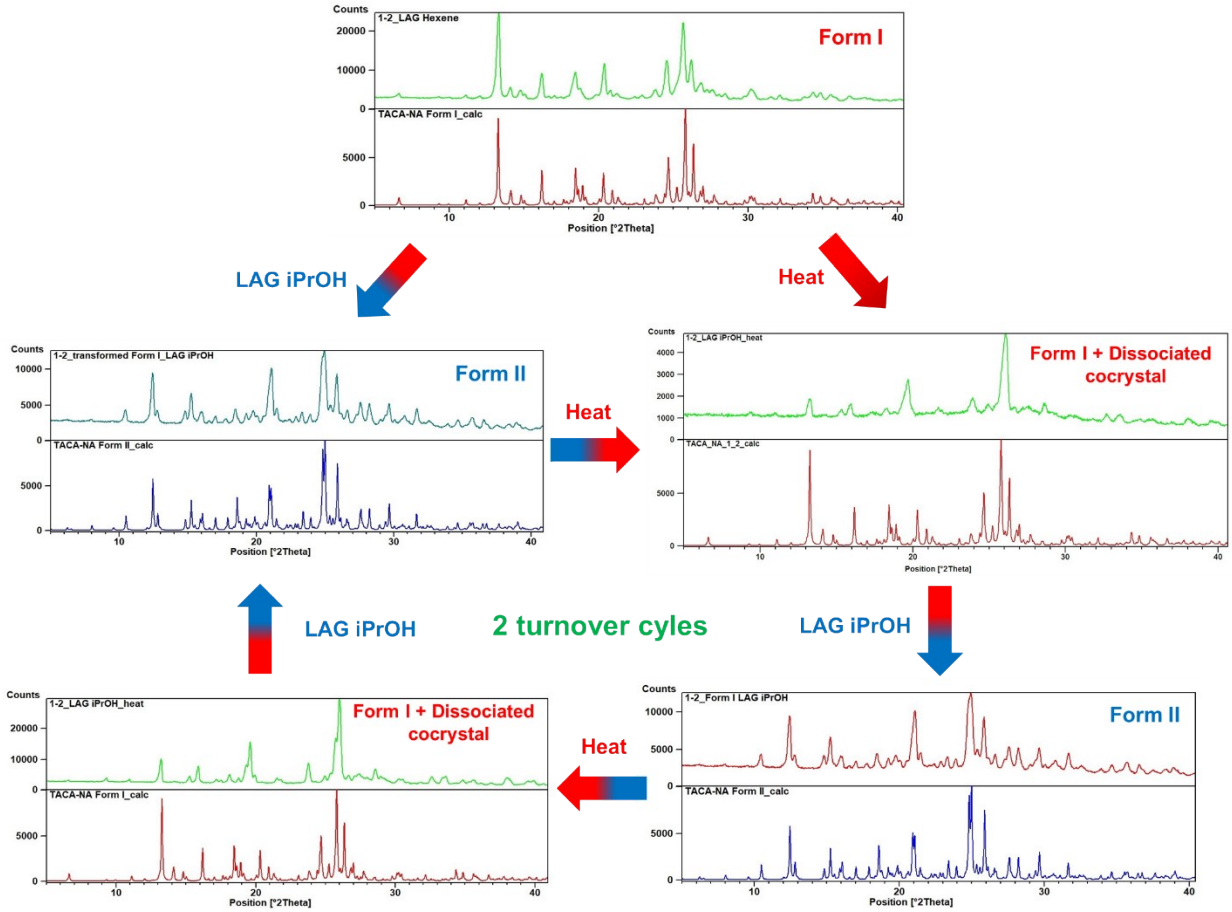

Figure S5. PXRD pattern showing the interconvertible nature of Form I and Form II of $(TACA)_2$•$(NA)_4$•(H_2O) along with dissociated cocrystal upon heating.

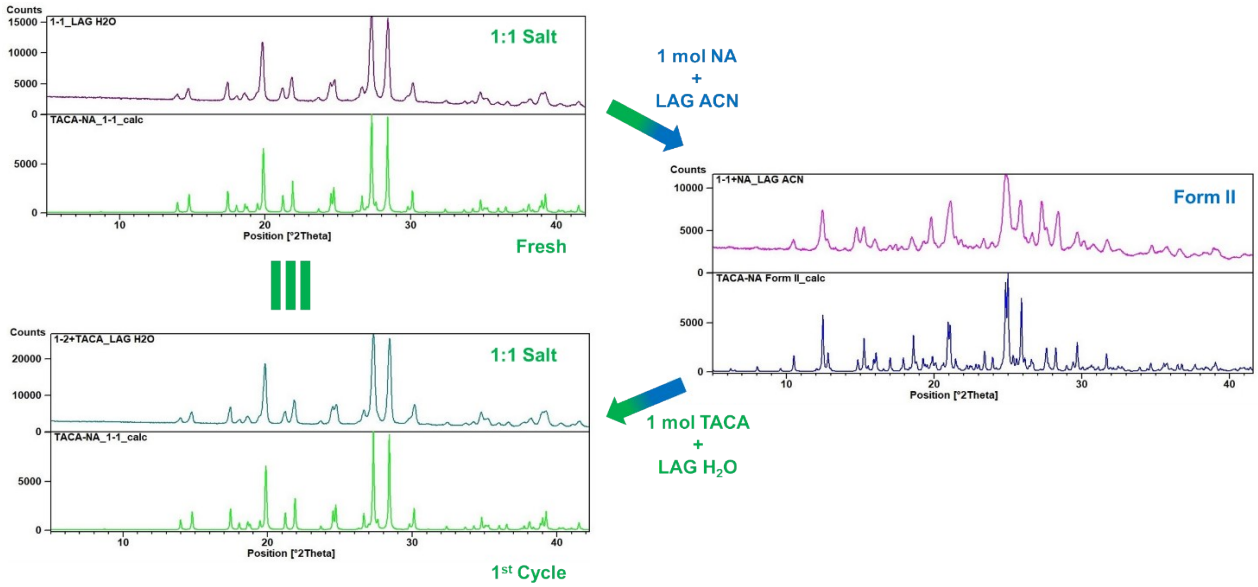

Figure S6. PXRD pattern showing the interconvertible nature of 1:1 molecular salt hydrate $(TACA)^{-}$ $\bullet(NA)^{+}\bullet(H_2O)$ and Form II of $(TACA)_2\bullet(NA)_4\bullet(H_2O)$ under specific condition mentioned in figure.

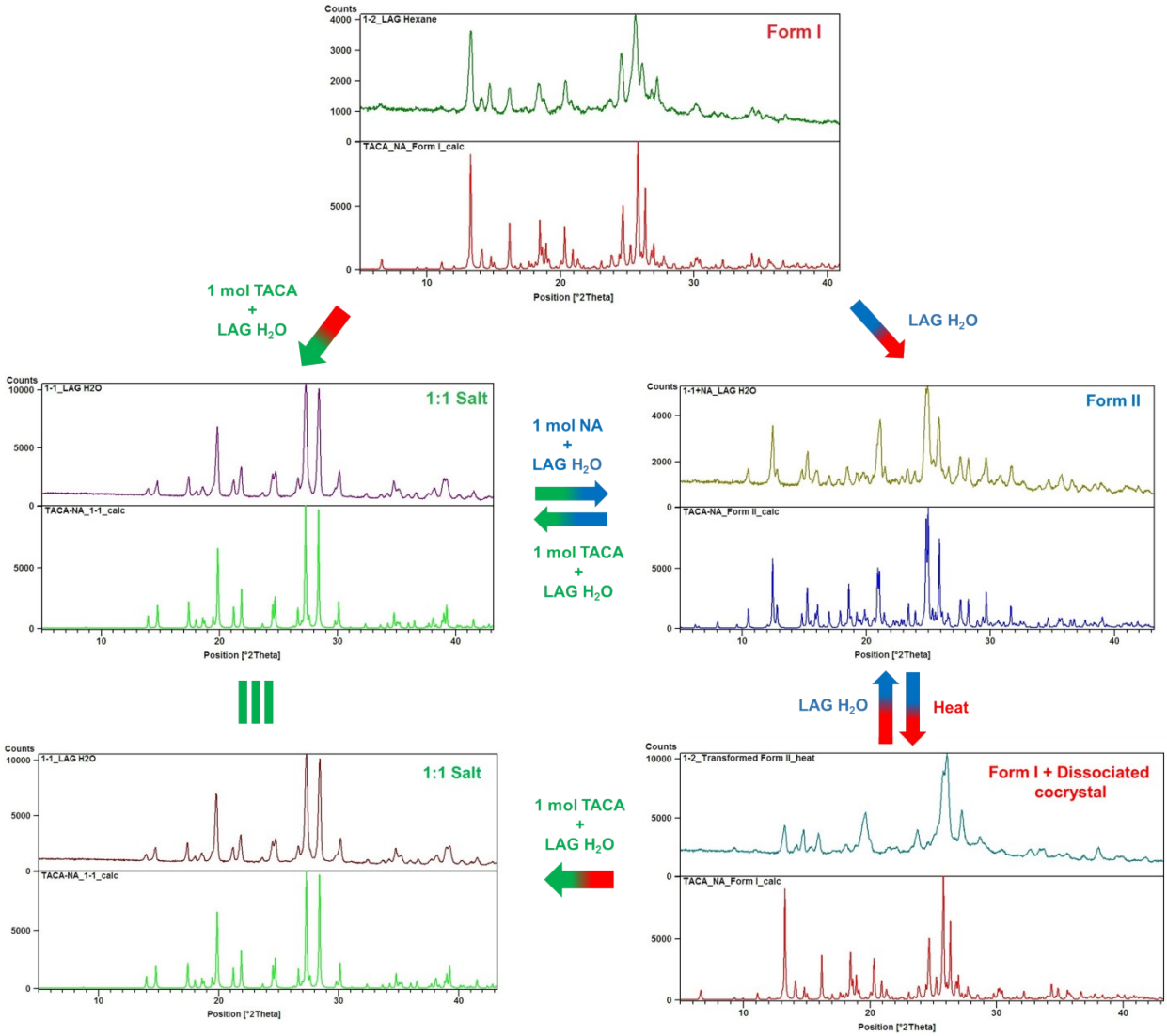

Figure S7. PXRD pattern showing the interconvertible nature of 1:1 molecular salt hydrate $(TACA)^{-}$ •$(NA)^{+}$•(H_2O), Form I and Form II of $(TACA)_2$•$(NA)_4$•(H_2O) along with dissociated cocrystal upon heating. Cocrystal dissociation is observed only in case of Form I showing its metastable nature compared to Form II.

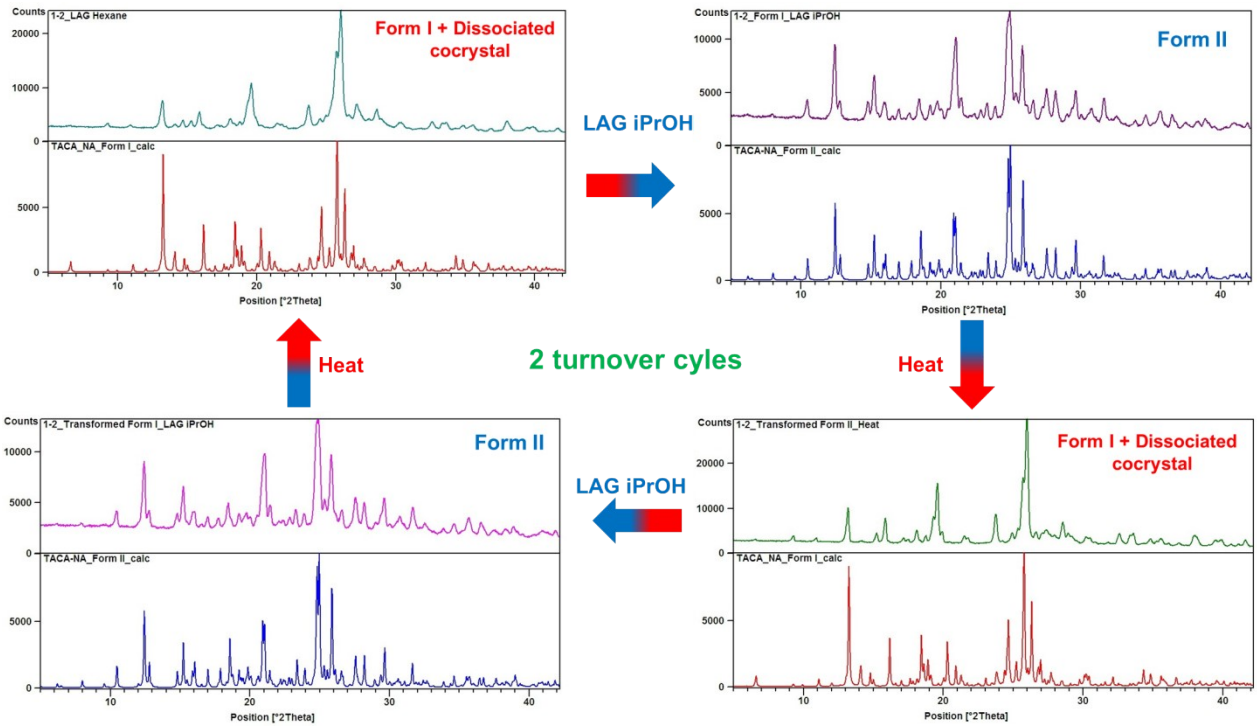

Figure S8. PXRD pattern showing the interconvertible nature of Form I and Form II of $(TACA)_2$•$(NA)_4$•(H_2O) along with dissociated cocrystal upon heating. Cocrystal dissociation is observed only in case of Form I showing its metastable nature compared to Form II.

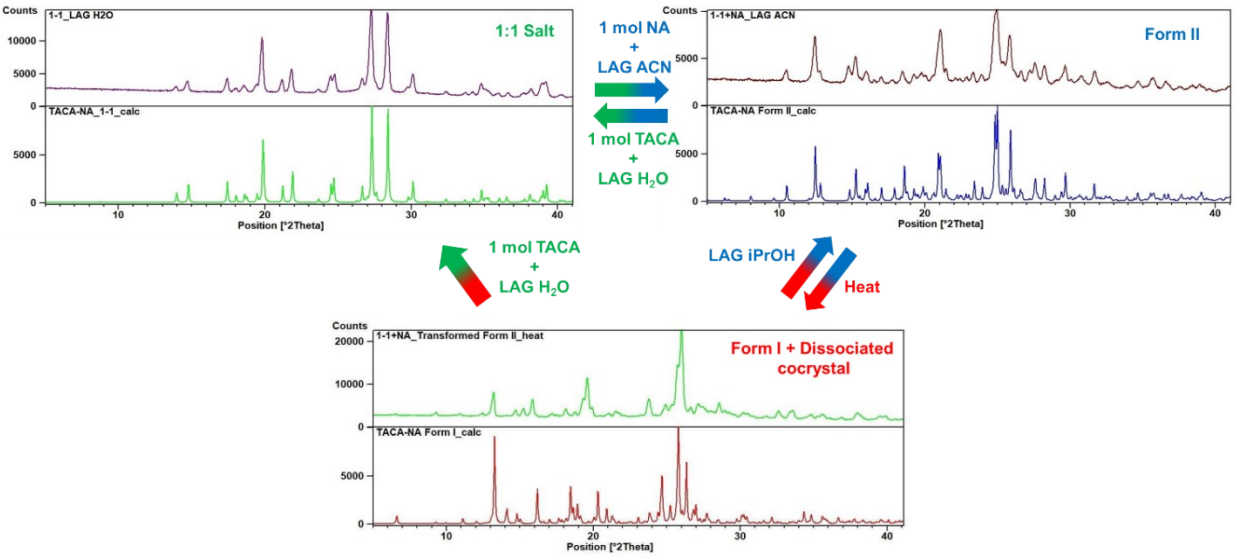

Figure S9. PXRD pattern showing the interconvertible nature of TACA-NA of the stoichiometric ratio 1:1 and 1:2.

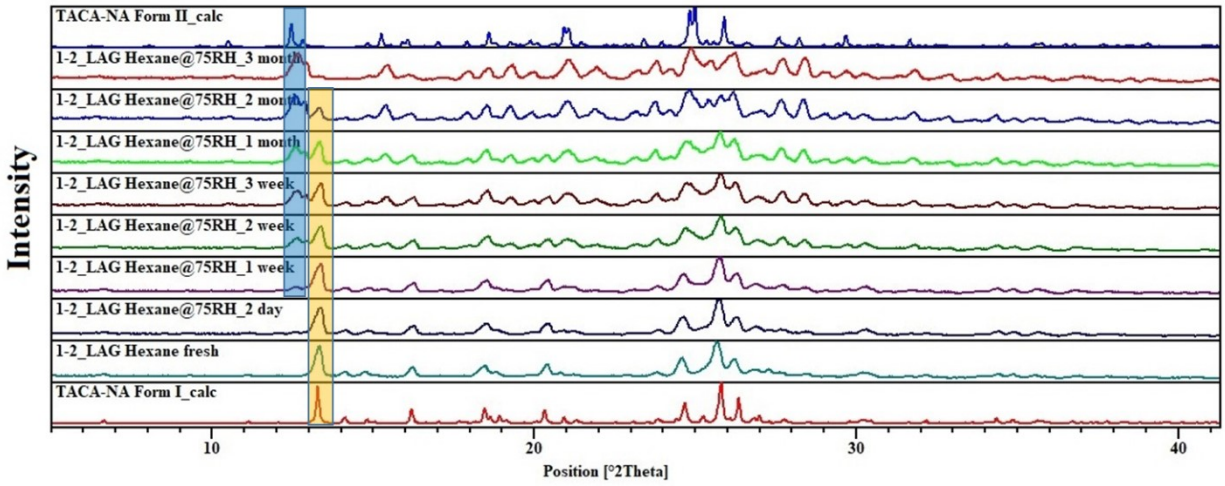

Figure S10. PXRD pattern of 1:2 TACA-NA Form I under 75% relative humidity placed for a period of 3 months showing polymorphic transformation from Form I to Form II. The characteristic peaks correspond to Form I and Form II are shown using yellow and blue highlights.

Rietveld refinement

Rietveld refinement[2] was performed in TOPAS Academic 7.24.[3] The peak shape functions were defined with a pseudo-Voigt function, with the addition of a simple axial divergence model. The background was modelled with a Chebyshev polynomial function with 4 terms. The refinement involved four crystal phases, namely Forms I and II of 1:2 $(TACA)_2•(NA)_4•(H_2O)$, 1:1 $(TACA)^-•(NA)^+•(H_2O)$ and TACA Form I (CSD TELZOZ).[4] The unit cell parameters and scale factors for all the individual phases were refined, and the final composition of the mixture was expressed in weight fractions.

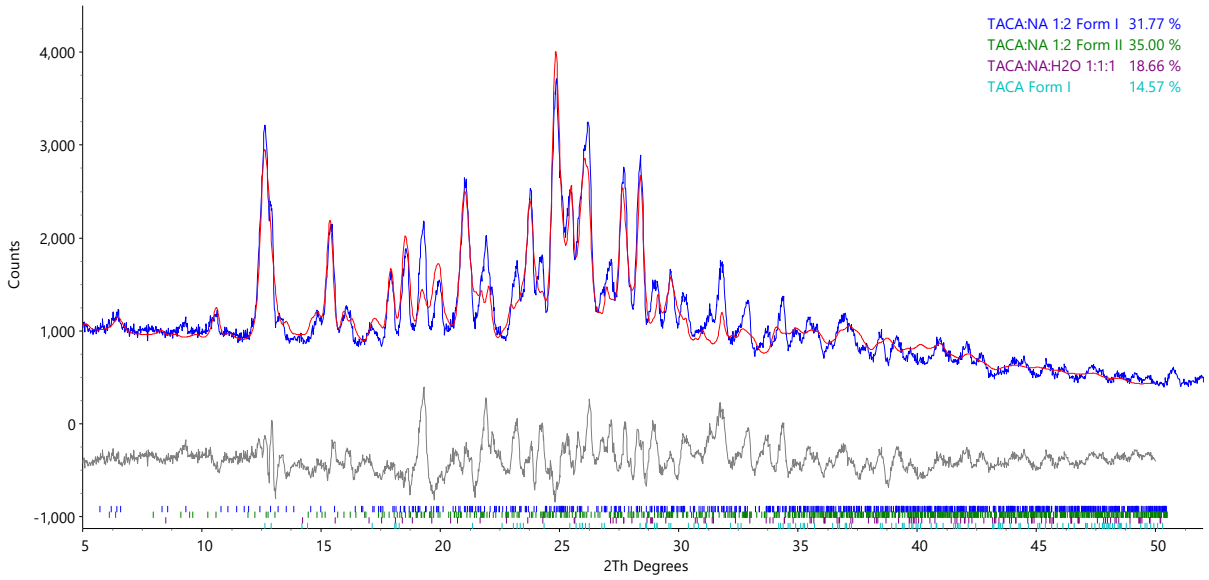

Figure S11. Rietveld refinement of powder pattern obtained after exposure of Form I powder sample under 75% RH for a period of 2.5 months shows transformation of Form I to Form II along with 1:1 molecular salt and starting material TACA.

Note: Broad peak and overlap of a few major peaks with Form I and Form II of $(TACA)_2•(NA)_4•(H_2O)$, 1:1 molecular salt hydrate $(TACA)^-•(NA)^+•(H_2O)$ and starting material may be the reason for imperfect match during Rietveld refinement and unassigned peaks left in difference map. Several round of grinding during the turnover experiment may be the reason for partial amorphization that resulted appearance of broad peaks with relatively poor intensity during our analysis.

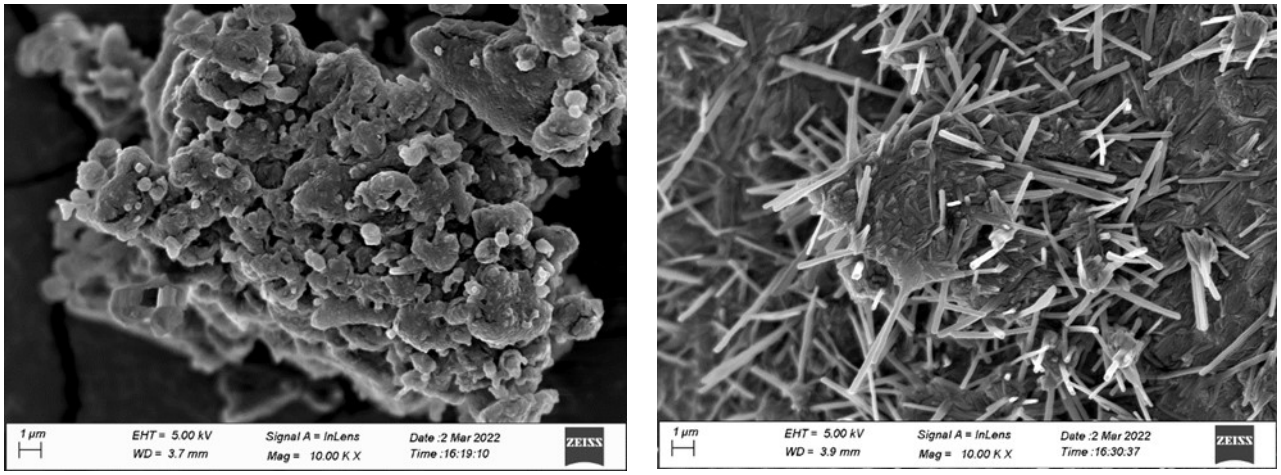

(a) (b)

Figure S12. SEM images of TACA-NA (a) 1:2 transformed Form I and (b) 1:2 transformed Form II.

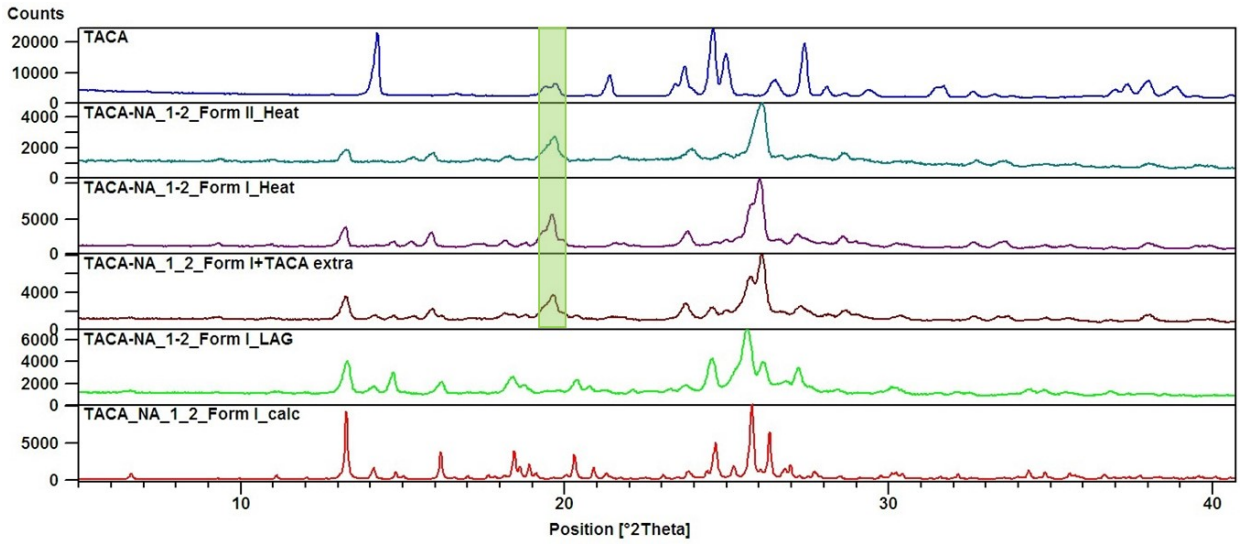

Figure S13. Comparison of PXRD patterns of heated 1:2 TACA-NA Form I and II, addition of trace amount of TACA in Form I cocrystal along with starting material TACA and calculated powder patterns of respective Form I, II shows appearance of new peaks corresponding to TACA highlighted in green that supports cocrystal dissociation.

4. Theoretical Calculations

Important intermolecular interactions within the crystal structure of Form I and Form II are identified through Hirshfeld surface analysis using Crystal Explorer 17.[5] The Hirshfeld surface is defined as a set of points in 3D space where the ratio of promolecule and procrystal electron densities equals 0.5. The exploration of intermolecular contacts is provided by mapping normalized contact distances (d_{norm}), which is a function of the closest distance from the point to the nuclei interior (d_i) and exterior (d_e) to the surface as well as on the van der Waals radii (r_{vdw}).[6] The percentage of interactions obtained from the Hirshfeld surface analysis is visualized in the Figure S14.

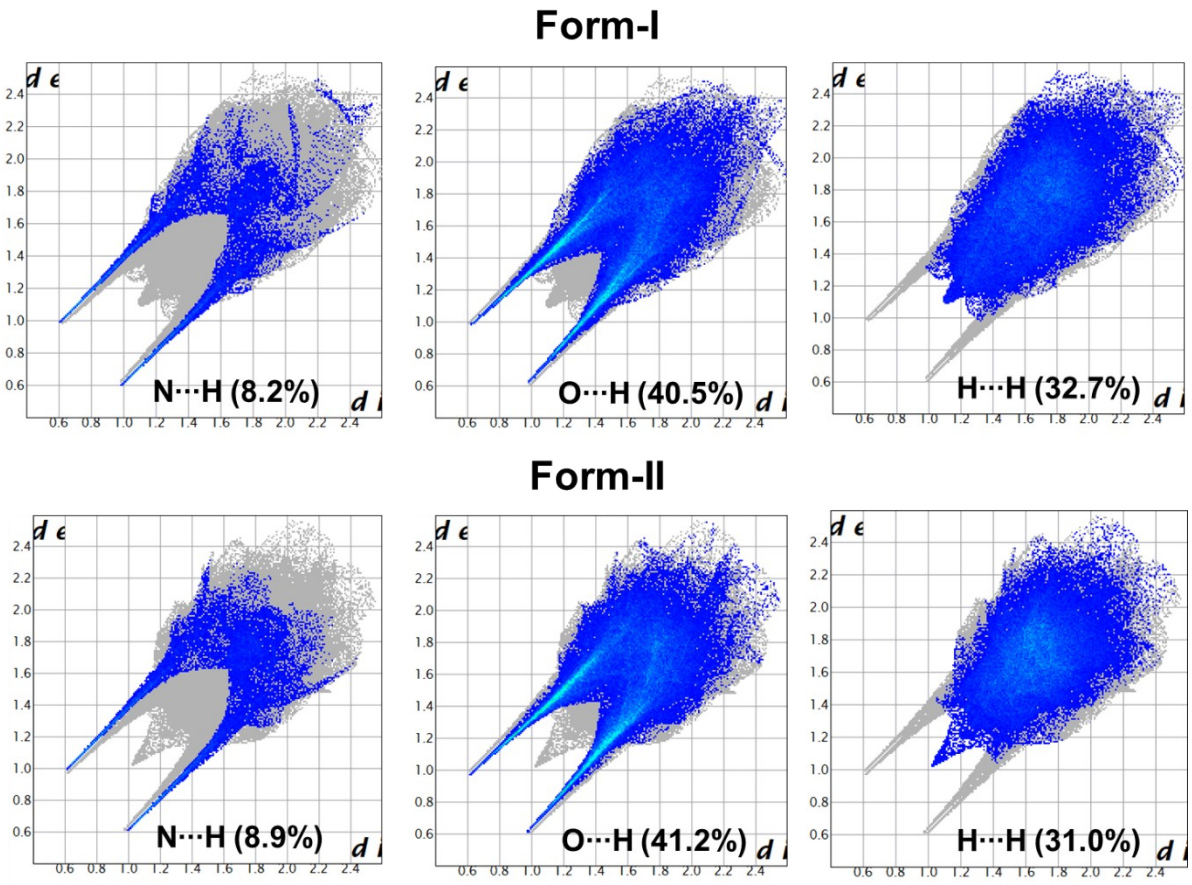

Figure S14. Contribution of various intermolecular interactions present in the two polymorphic forms of TACA-NA cocrystal hydrate based on Hirshfeld surface analysis.

For p*K*a calculations we have used Density Functional Theory to optimize the geometries at wb97xd/6-311++G** level of theory and employing ultrafine numerical integration grid (pruned 99,590). To optimize the solvated counterparts, the effect of solvent polarity is considered using the SMD [scrf = (smd, solvent=water)] implicit continuum solvation model as implemented in Gaussian16.[7] The pKa values are calculated following the protocol described in literature.[8,9]

Packing energies for polymorphs (with normalized H-atom positions) were obtained after geometry optimization performed using the Forcite module of Materials studio (version 7.0) software using Dreiding force field with Gasteiger atomic charges. The unit cell parameters and motion groups were kept fixed during optimization. The invariant valence terms are ignored and only the packing energies were obtained after optimization. Valance terms for unit cell contents (with normalized H-atom positions) were obtained separately using more accurate Gaussian09 computations and added to packing energies for computing the final stability differences between polymorphs.

The lattice energy values are calculated at B3LYP-GD3/Def2TZVP level of theory. The dispersion parameter GD3 is employed since it is capable of describing the dispersion effects in molecules as well as aggregates.

Non-covalent interactions (NCI) plot: As non-covalent interactions predominantly govern the molecular arrangement and stability in the organic molecular system, we tried to address this by qualitatively visualizing different non-covalent interactions in both Form I and Form II. We visualized the NCI plot using the open-source code VMD[6] and Multiwfn.[7]

5. Optimized coordinates of the structures for p*K*a calculations

a) TACA (gas phase)

Sum of electronic and thermal Energies = -683.476701 a.u. = -428881.6299 kCalmol^{-1}

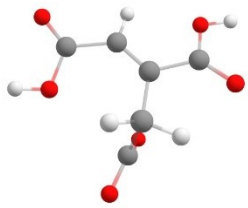

18

$C_6H_6O_6$

C	-0.230317000	-1.989610000	-0.084398000
O	-0.818847000	-2.990463000	0.215492000
O	0.154897000	-1.715771000	-1.342216000
H	-0.128951000	-2.453286000	-1.895494000
C	0.202875000	-0.930851000	0.907121000
H	1.096536000	-1.326278000	1.396961000
H	-0.586119000	-0.859185000	1.652159000
C	0.535768000	0.410375000	0.312912000
C	2.005059000	0.664179000	0.136123000
O	2.859349000	-0.100835000	0.500398000
O	2.286555000	1.827320000	-0.467391000

H	3.246553000	1.891740000	-0.527331000
C	-0.328249000	1.363718000	-0.050951000
H	0.042386000	2.303188000	-0.439526000
C	-1.808109000	1.318139000	0.016711000
O	-2.498197000	2.290369000	-0.142384000
O	-2.315715000	0.095828000	0.251401000
H	-3.276895000	0.176543000	0.265725000

b) TACA (SMD=water)

Sum of electronic and thermal Energies = -683.507353 a.u. = -428900.864 kCalmol^{-1}

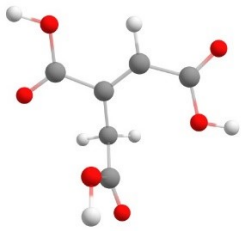

18

$C_6H_6O_6$

C	0.059266000	1.998713000	0.009069000
O	-0.389199000	3.070660000	-0.334731000
O	0.465766000	1.750339000	1.252701000
H	0.342294000	2.545834000	1.791067000
C	0.246210000	0.842050000	-0.940018000
H	1.120263000	1.094109000	-1.546217000
H	-0.614081000	0.831245000	-1.606866000
C	0.454632000	-0.498500000	-0.292895000
C	1.884668000	-0.907891000	-0.112870000
O	2.813894000	-0.174540000	-0.374570000
O	2.046997000	-2.138272000	0.366503000

H	2.993651000	-2.314499000	0.464393000
C	-0.511348000	-1.323068000	0.120915000
H	-0.263862000	-2.294165000	0.530472000
C	-1.970426000	-1.081600000	0.029520000
O	-2.765060000	-1.992022000	-0.082647000
O	-2.330209000	0.195747000	0.105045000
H	-3.293795000	0.263966000	0.026409000

c) TACA-Anion (gas phase)

Sum of electronic and thermal Energies = -682.954412 a.u. = -428553.8935 kCalmol^{-1}

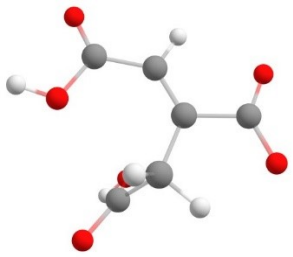

17

$C_6H_5O_6$

C	-0.799338000	1.769346000	0.109361000
O	-1.576389000	2.609267000	-0.279487000
O	-0.695944000	1.471649000	1.418420000
H	-1.329378000	2.039875000	1.869914000
C	0.172585000	1.030840000	-0.762972000
H	1.029639000	1.701565000	-0.911382000
H	-0.320839000	0.888132000	-1.725259000
C	0.763078000	-0.250624000	-0.238535000
C	2.321425000	-0.239213000	-0.030881000
O	2.867570000	0.840745000	-0.337053000

O	2.816050000	-1.291645000	0.399171000
C	0.096982000	-1.382400000	0.027636000
H	0.679973000	-2.219988000	0.393332000
C	-1.337797000	-1.637952000	-0.080615000
O	-1.887141000	-2.670122000	0.242638000
O	-2.071090000	-0.614205000	-0.592062000
H	-2.985459000	-0.915082000	-0.583593000

d) TACA-Anion (SMD=water)

Sum of electronic and thermal Energies = -683.0664 a.u. = -428624.166 kCalmol^{-1}

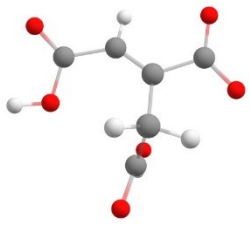

17

$C_6H_5O_6$

C	0.106869000	1.954563000	-0.004957000
O	-0.287289000	3.037202000	-0.385517000
O	0.391224000	1.704913000	1.272660000
H	0.234562000	2.506656000	1.792643000
C	0.360212000	0.796621000	-0.934684000
H	1.284854000	1.044940000	-1.461613000
H	-0.444592000	0.801952000	-1.668923000
C	0.504846000	-0.554742000	-0.289365000
C	1.934402000	-1.060499000	-0.059618000
O	2.831207000	-0.182804000	-0.056337000
O	2.103855000	-2.289326000	0.122681000

C -0.509941000 -1.328791000 0.110793000

H -0.293847000 -2.310513000 0.514810000

C -1.951701000 -1.033811000 0.039269000

O -2.799990000 -1.904530000 0.112744000

O -2.266521000 0.256103000 -0.091154000

H -3.228994000 0.344458000 -0.146163000

e) Water

Sum of electronic and thermal Energies = -76.407825 a.u. = -47945.91019 $kCalmol^{-1}$

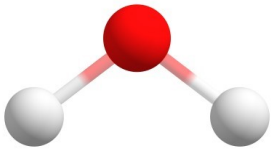

3

H2O

O 0.000000000 0.000000000 0.116281000

H 0.000000000 -0.760662000 -0.465124000

H 0.000000000 0.760662000 -0.465124000

f) Hydronium ion

Sum of electronic and thermal Energies = -76.671707 a.u. = -48111.49614 $kCalmol^{-1}$

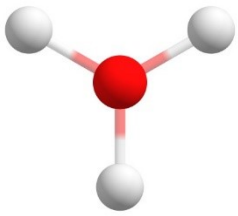

4

H_3O

O 0.000000000 0.000000000 0.000000000

H 0.000000000 0.970369000 0.000000000

H	0.840365000	-0.485185000	0.000000000
H	-0.840365000	-0.485185000	0.000000000

g) NA (gas phase)

Sum of electronic and thermal Energies = -416.836977 a.u. = -261565.2031 kCalmol^{-1}

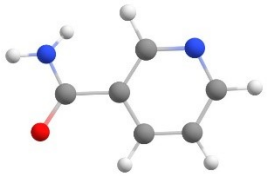

15

$C_6N_2H_6O$

C	2.509394000	-0.136098000	0.012259000
C	1.921287000	1.116199000	0.158757000
C	0.539914000	1.203544000	0.139804000
C	-0.203667000	0.036364000	-0.012355000
C	0.488484000	-1.163013000	-0.169834000
N	1.815846000	-1.259714000	-0.158143000
H	0.021809000	2.150610000	0.236019000
H	3.590386000	-0.241339000	0.026135000
H	2.537931000	1.998113000	0.281905000
H	-0.044368000	-2.094834000	-0.342707000
C	-1.700854000	0.142448000	-0.035149000
O	-2.257888000	1.184266000	-0.315970000
N	-2.390763000	-0.996270000	0.261641000
H	-3.392966000	-0.916992000	0.318773000
H	-1.952616000	-1.774470000	0.722252000

h) NA (SMD=water)

Sum of electronic and thermal Energies = -416.859012 a.u. = -261579.03 kCalmol^{-1}

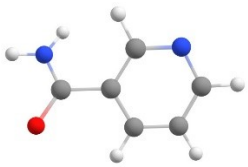

15

$C_6N_2H_6O$

C	2.508146000	-0.134255000	0.002279000
C	1.922046000	1.109974000	0.191203000
C	0.540309000	1.199636000	0.178142000
C	-0.204787000	0.037961000	-0.007343000
C	0.479835000	-1.160174000	-0.195242000
N	1.810662000	-1.256708000	-0.195950000
H	0.040424000	2.150951000	0.317447000
H	3.588393000	-0.234449000	0.006646000
H	2.540155000	1.985706000	0.343738000
H	-0.059679000	-2.084507000	-0.375867000
C	-1.698255000	0.126395000	-0.036829000
O	-2.258738000	1.163386000	-0.406104000
N	-2.382465000	-0.957571000	0.352439000
H	-3.391069000	-0.929711000	0.333339000
H	-1.929457000	-1.772348000	0.734842000

i) NA-H (gas phase)

Sum of electronic and thermal Energies = -417.189178 a.u. = -261786.2092 $kCalmol^{-1}$

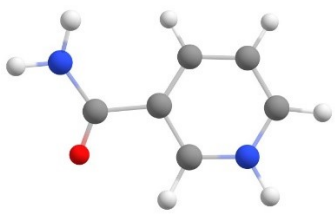

16

$C_6N_2H_7O$

C	2.521094000	0.046062000	0.007843000
C	1.849202000	1.235675000	-0.140945000
C	0.454697000	1.232687000	-0.139156000
C	-0.246541000	0.039980000	0.011284000
C	0.475352000	-1.133382000	0.139422000
N	1.814080000	-1.094174000	0.142263000
H	-0.073790000	2.169035000	-0.280495000
H	3.599079000	-0.042276000	0.019350000
H	2.409157000	2.152910000	-0.263727000
H	-0.012357000	-2.097136000	0.223468000
C	-1.756000000	-0.128997000	-0.032166000
O	-2.202858000	-1.213085000	-0.326307000
N	-2.497037000	0.964561000	0.241008000
H	-3.500300000	0.854542000	0.233303000
H	-2.124565000	1.790954000	0.676001000
H	2.319508000	-1.968216000	0.241960000

j) NA-H (SMD=water)

Sum of electronic and thermal Energies = -416.859012 a.u. = -261579.03 kCalmol^{-1}

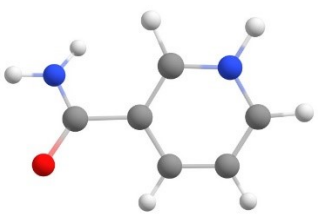

16

$C_6N_2H_7O$

C	2.511294000	-0.026476000	0.016842000
C	1.873010000	1.176701000	0.217585000
C	0.486333000	1.213044000	0.196557000
C	-0.244403000	0.041589000	-0.001477000
C	0.440498000	-1.139173000	-0.200997000
N	1.780552000	-1.132009000	-0.189285000
H	-0.037936000	2.150131000	0.339590000
H	3.584753000	-0.149125000	0.008312000
H	2.457671000	2.070668000	0.382286000
H	-0.027400000	-2.095866000	-0.389457000
C	-1.745690000	0.113514000	-0.044217000
O	-2.292003000	1.126037000	-0.480039000
N	-2.416144000	-0.950291000	0.406801000
H	-3.425388000	-0.934602000	0.380208000
H	-1.958709000	-1.738030000	0.839484000
H	2.265928000	-2.010572000	-0.348487000

Supporting Information References

1. B. Golec, P. Das, M. Bahou and Y.-P. Lee, *J. Phys. Chem. A*, **2013**, 117, 50, 13680–13690.
2. H. M. Rietveld, *J. Appl. Cryst*. **1969**, 2, 65-71.
3. A. A. Coelho, *J. Appl. Cryst.* **2018**, 51, 210-218.
4. N. Nagel, U. Endruschat, H. Bock, *Acta Crystallogr. Section C*, **1996**, 52, 2912-2915.
5. M. J. Turner, J. J. McKinnon, S. K. Wolff, D. J. Grimwood, P. R. Spackman, D. Jayatilaka, & M. A. Spackman, CrystalExplorer[17] (**2017**). University of Western Australia. http://hirshfeldsurface.net
6. M. A. Spackman and D. Jayatilaka, *CrystEngComm*, **2009**, 11, 19-32.

7. Gaussian 16, Revision B.01, M. J. Frisch, G. W. Trucks, H. B. Schlegel, G. E. Scuseria, M. A. Robb, J. R. Cheeseman, G. Scalmani, V. Barone, G. A. Petersson, H. Nakatsuji, X. Li, M. Caricato, A. V. Marenich, J. Bloino, B. G. Janesko, R. Gomperts, B. Mennucci, H. P. Hratchian, J. V. Ortiz, A. F. Izmaylov, J. L. Sonnenberg, D. Williams-Young, F. Ding, F. Lipparini, F. Egidi, J. Goings, B. Peng, A. Petrone, T. Henderson, D. Ranasinghe, V. G. Zakrzewski, J. Gao, N. Rega, G. Zheng, W. Liang, M. Hada, M. Ehara, K. Toyota, R. Fukuda, J. Hasegawa, M. Ishida, T. Nakajima, Y. Honda, O. Kitao, H. Nakai, T. Vreven, K. Throssell, J. A. Montgomery, Jr., J. E. Peralta, F. Ogliaro, M. J. Bearpark, J. J. Heyd, E. N. Brothers, K. N. Kudin, V. N. Staroverov, T. A. Keith, R. Kobayashi, J. Normand, K. Raghavachari, A. P. Rendell, J. C. Burant, S. S. Iyengar, J. Tomasi, M. Cossi, J. M. Millam, M. Klene, C. Adamo, R. Cammi, J. W. Ochterski, R. L. Martin, K. Morokuma, O. Farkas, J. B. Foresman, and D. J. Fox, Gaussian, Inc., Wallingford CT, **2016**.

8. Humphrey, W.; Dalke, A.; Schulten, K. VMD: Visual Molecular Dynamics. *J. Mol. Graphics*, **1996**, 14, 33-38.
9. Lu, T.; Chen, F. Multiwfn: A Multifunctional Wavefunction Analyzer. *J. Comput. Chem.* **2012**, 33, 580-592.